Polymer Vol. 39 No. 24 pp. 6127–6135, 1998
0032-3861/98/$ – see front matter

PII: S0032-3861(98)00102-5

Structural characterization of ultrahigh-molecular-weight polyethylene reactor powders based on fuming nitric acid etching

Hiroki Uehara[a]†, Mitsuhiro Nakae[a], Tetsuo Kanamoto[a,*], Osamu Ohtsu[b], Akira Sano[c] and Kazuo Matsuura[c]

[a]*Department of Applied Chemistry, Science University of Tokyo, Kagurazaka, Shinjuku-ku, Tokyo 162, Japan*
[b]*Central Technical Research Laboratory, Nippon Oil Co. Ltd., 8 Chidori-cho, Naka-ku, Yokohama 231, Japan*
[c]*Japan Polyolefins Co. Ltd., 10-1 Chidori-cho, Kawasaki-ku, Kawasaki 210, Japan*
(Received 15 October 1997; revised 27 December 1997; accepted 29 January 1998)

A series of ultrahigh-molecular-weight polyethylenes with comparable viscosity-average molecular weights of around 2×10^6 has been prepared by using a high-activity Ziegler catalyst at different temperatures (T_{poly}) in the range 20–90°C, in hexane. The ductility and morphology of the nascent reactor powders have been studied. With decreasing T_{poly}, the drawability of the reactor powders increased significantly. The morphology of the samples has been characterized by scanning electron microscopy, wide-angle X-ray diffraction and the d.s.c. melting behaviour. On mild etching of the powders with fuming nitric acid at room temperature, more than 1 year was required to obtain fully etched morphologies. The selective removal of amorphous regions was confirmed. Extended fibrils (40–150 nm wide and 1–10 μm long) connecting globular particles (2–5 μm in diameter), the amount of which increased with T_{poly}, were also rapidly etched and disappeared. Both orthorhombic and monoclinic crystals survived even after prolonged treatment (9 months or more). No significant differences in the d.s.c. melting characteristics were observed for the series of reactor powders, which was primarily due to a rapid reorganization during the d.s.c. heating scans. However, the effect of T_{poly} on the morphology of the reactor powders was reflected in the melting characteristics of the etched samples. Etching proceeded more rapidly for the powders prepared at higher T_{poly}, although initial crystallinities were comparable for all samples. This suggests that the nature of the amorphous regions depends on T_{poly}. The crystal thicknesses of the initial powders, evaluated from the melting temperatures of fully etched samples, increased with T_{poly}. These results suggest that polymer segments crystallize near T_{poly} after having grown longer than a certain length during polymerization. The effect of T_{poly} on the ductility of the reactor powders is also discussed, based on morphological features revealed by the etching.

(Keywords: UHMW-PE reactor powders; ductility; morphology)

INTRODUCTION

High-performance polyethylene (PE) has been commercially produced by uniaxial drawing from gel-spun fibres[1] of ultrahigh-molecular-weight polyethylene (UHMW-PE)[2]. On the drawing of such solution-crystallized UHMW-PE, a reduced entanglement density improves sample ductility[3]. Single crystal mats of UHMW-PE, precipitated from dilute solutions, could be effectively superdrawn to a draw ratio (DR) of over 300[4] due to their minimized entanglement density and regular chain folding. The resultant tensile moduli of such superdrawn films were about 220 GPa[4], which is close to the X-ray crystal modulus along the chain axis (235 GPa)[5].

Certain nascent UHMW-PE powders also have fewer entanglements. Indeed, powder films compacted below the melting temperature (T_m) could be successfully ultradrawn to $DR < 85$ by applying a two-stage draw technique[6,7], *i.e.* a combination of first-stage solid-state coextrusion[8] followed by second-stage tensile draw[4]. Such highly drawn films exhibited tensile moduli of around 150 GPa[7,9,10]. Independently, Smith and co-workers[11–13] have reported the ultradrawing of virgin UHMW-PE prepared by use of a low-activity catalyst. The drawability and the resultant tensile properties of the drawn products were significantly affected by the polymerization conditions[9,12–14]. It was also shown that some specific powders could be effectively ultradrawn in the crystalline state, even above their static T_m (about 140°C)[10].

It has been reported that virgin PE powders have a unique morphology. The most minimized crystalline texture in the powder is made up of lamellae having thicknesses of 20–30 nm along the chain direction and widths of 7–15 nm perpendicular to the chain direction, as analyzed by scanning electron microscopy (SEM), pulsed NMR and X-ray diffraction[15]. Such lamellar crystals have ribbon- or noodle-like textures and fibrous structures[15–19]. The ribbons and noodles are folded into a submicron-sized particle, and oriented fibrils connect particles (2–10 μm in diameter) that consist of an assembly of the submicron-sized particles. The powder, around 50–300 μm in diameter[20], is composed of these particles. Such a unique powder structure is formed on crystallization during the polymerization[21].

* To whom correspondence should be addressed. Fax: 00 81 3 3253 2214; e-mail: tkanamot@ch.kagu.sut.ac.jp
† Present address: Department of Materials Science, Gunma University, 1-5-1 Tenjin, Kiryu, Gunma 376, Japan

Generally, fuming nitric acid etching selectively oxidizes and removes amorphous regions of the PE samples, including lamellae folds[21]. However, conventional etching[22] around 70°C etches even the crystalline region on prolonged treatment[21]. Gradual changes in the sample morphology may be better followed by mild etching at room temperature, especially at the earlier stage.

In this work, the ductility and morphology of a series of UHMW-PE reactor powders, prepared at different temperatures (T_{pol}) using a high-activity Ziegler catalyst, have been studied. To examine the effect of the polymerization conditions on the morphology of the reactor powders, fuming nitric acid etching was carried out at room temperature for 2 years or less. The etching behaviour and the powder morphologies, before and after etching, have been analyzed by d.s.c., SEM and X-ray diffraction measurements.

EXPERIMENTAL

Materials

A series of nascent UHMW-PE reactor powders was prepared at the Nippon Oil Company Ltd. by the polymerization of ethylene in hexane at $T_{poly} = 20 - 90$°C and at an ethylene pressure of 11 atm, using a high-activity Ziegler catalyst. The temperature of the reaction medium was taken as T_{poly}. The viscosity-average molecular weight, M_v, of UHMW-PE was controlled by the addition of a small amount of hydrogen gas, depending on T_{poly}. These samples had comparable M_v values of around 2×10^6.

Etching treatment by fuming nitric acid

The fuming nitric acid etching of the reactor powders was performed at room temperature for 1 week to 2 years. An excess amount (10 ml) of fuming nitric acid with a density of 1.52 g cm^{-3} was added to 0.2 g of a powder sample contained in a glass sample tube. The sample tube assembly was stored in a desiccator to avoid the evaporation of fuming nitric acid. Every 1–2 months, the nitric acid was replaced with fresh acid. After treatment for the given period of time, the sample was recovered by filtration through a glass filter, washed by distilled water and hot acetone, and dried well at room temperature *in vacuo*.

Drawing

The ductility of the nascent powders was determined by a two-stage draw[7]. For this, the powders were compression-moulded into films at 130°C (about 10°C below their d.s.c. peak melting temperatures (T_m)) and at 12 MPa for 30 min. A strip ($3 \times 0.3 \times 50$ mm^3) cut from the compacted powder film was sandwiched between split billet halves of high-density PE, and the assembly was co-extruded at 125°C to a low extrusion draw ratio (*EDR*) of 6. For the second-stage draw, the extrudate was drawn by a tensile force at a constant temperature (T_d) of 145°C and constant cross-head speeds, corresponding to an initial strain rate of 2 min^{-1}, in the Tensilon tensile tester RTM-100 equipped with an air oven. The total *DR* (DR_t) was defined by $DR_t = (\text{initial } EDR) \times (\text{second} - \text{stage tensile } DR)$.

Measurements

The polymerized and etched powders were characterized by d.s.c. measurements. The first heating run involved scanning from 80 to 180°C at 3°C min^{-1}. The sample was then slowly cooled to room temperature in a d.s.c. pan. The second reheating run was also carried at 3°C min^{-1}. All scans were performed under a nitrogen gas flow. The T_m of each sample was evaluated from the postion of the peak in the endotherm. Crystallinities were calculated from the heats of fusion (ΔH_f), assuming an enthalpy of fusion for a perfect PE crystal of 290 J g^{-1}[23]. The sample sizes were 0.1 mg and 1 mg for the determinations of T_m and ΔH_f, respectively. The above d.s.c. melting characteristics were calibrated using an indium standard.

Wide-angle X-ray diffraction (WAXD) profiles were recorded with use of the Rigaku X-ray diffractometer RAD-IIIA equipped with a pulse-height discriminator. Some WAXD profiles were recorded using a Rigaku RINT-1400 X-ray diffractometer. Cu Kα radiation monochromatized with a nickel filter or a graphite monochromator was used. The half-width of the orthorhombic (002) reflection was used to estimate the crystallite size along the chain axis, D_{002}, applying the Scherrer equation assuming no significant crystal disorder along the chain axis[24]. SEM observations were made by use of a Hitachi-type S-5000 scanning electron microscope operated at 5 kV.

Table 1 Polymerization temperatures (T_{poly}), sample M_v, and d.s.c. characteristics of a series of reactor powders prepared by use of a high-activity Ziegler catalyst at T_{poly} in the range 20–90°C

Sample	T_{poly} (°C)	$10^{-6} M_v$	T_m (°C)	χ_c^a (%)
1	20	2.0	140	65
2	40	1.8	140	65
3	60	2.2	141	67
4	80	1.9	141	68
5	90	1.7	141	67

[a]The crystallinity, χ_c, was calculated from the heat of fusion, assuming an enthalpy of fusion for a perfect PE crystal of 290 J g^{-1}[23]

RESULTS AND DISCUSSION

Characteristics and ductility of nascent powders

The M_v, T_m and crystallinity (χ_c) values, calculated from the sample ΔH_f, are summarized in *Table 1* for a series of reactor powders polymerized at 20–90°C using a high-activity Ziegler catalyst. The T_m and χ_c values stayed almost constant at 140–141°C and 65–68%, respectively, independent of T_{poly}.

The effect of T_{poly} on the drawability of the reactor powders was examined. The powder films compacted at 130°C, below the static T_m, were too brittle to be drawn directly by a tensile force. However, they were ductile after having been drawn to a low *EDR* of 6. Thus, the extrudates were further drawn by a second-stage tensile draw at 145°C. The draw proceeded in the crystalline state, as reported by time-resolved WAXD measurements during drawing[10]. The maximum DR_t achieved by the two-stage draw are shown in *Figure 1* as a function of T_{poly}. The drawability of the nascent powders increased significantly with decreasing T_{poly}. A similar effect of T_{poly} on the powder ductility was also observed by Rotzinger *et al.*[13] for UHMW-PE prepared using a low-activity Ziegler catalyst. The maximum tensile modulus and strength achieved increased with decreasing T_{poly}, reflecting the improved drawability of the samples. For the most ductile powder, synthesized at 20°C in this work, the highest tensile modulus and strength achieved were 110 and 1.5 GPa, respectively, at a maximum achieved draw ratio of 85.

The sample ductility is primarily controlled by the

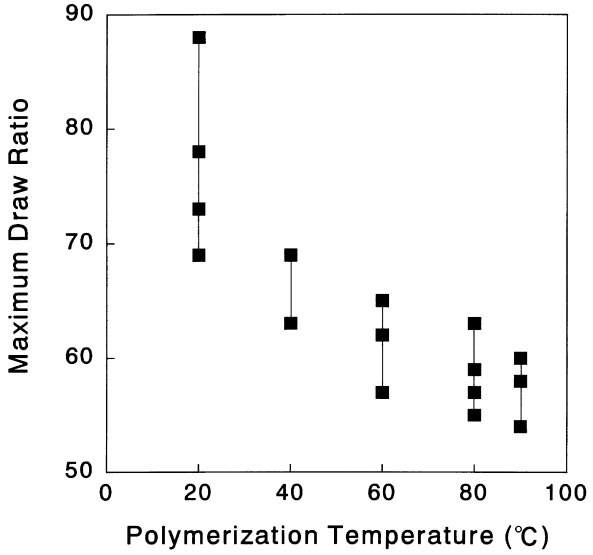

Figure 1 Effect of polymerization temperature on the maximum DR_t achieved for a series of UHMW-PE reactor powders prepared with use of a high-activity Ziegler catalyst and having comparable M_v values of about 2×10^6

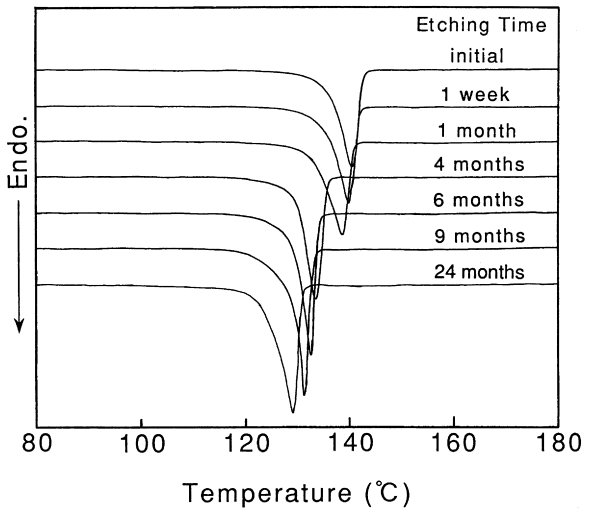

Figure 2 Changes in the d.s.c. thermogram of sample 2 ($T_{poly} = 20$°C) on fuming nitric acid treatment. Etching was performed at room temperature

entanglements existing in amorphous regions, since PE crystals are ductile[3]. Highly entangled UHMW-PE displays low crystallinity and low ductility, as illustrated by melt-crystallized UHMW-PE. Thus, a sample exhibiting higher ductility may be expected to have a higher χ_c. However, in spite of a significant increase in the drawability with decreasing T_{poly}, all the reactor powders showed comparable χ_c values of around 65%, estimated from the d.s.c. ΔH_f, independent of T_{poly}. Nevertheless, the origin of such a difference in drawability must be related to the specific morphology of the powders, as discussed below.

Etching behaviour analyzed by d.s.c. measurements

To study the effect of T_{poly} on the morphology, and hence the ductility, each reactor powder was gently etched by fuming nitric acid at room temperature.

Figure 2 compares the d.s.c. thermograms recorded for the first heating scans of sample 2 etched for various periods of time. All the reactor powders used in this work displayed a single endotherm, before and after etching. The peak

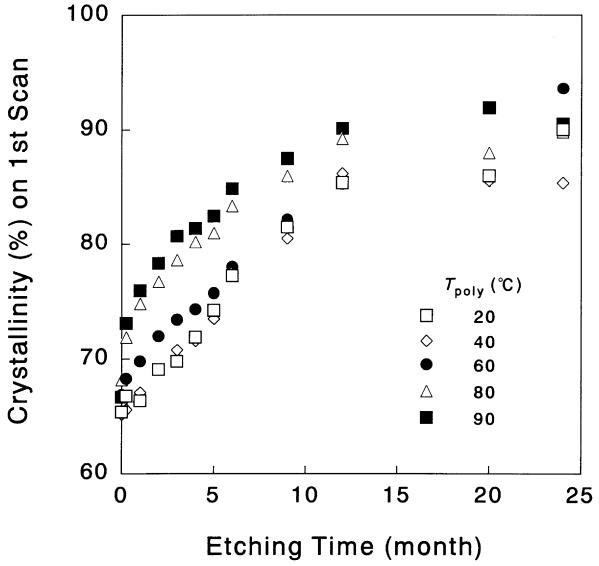

Figure 3 The crystallinity, calculated from the heat of fusion for the first heating scan, as a function of fuming nitric acid etching time for samples 1–5 polymerized at 20–90°C

gradually became sharper and the peak position shifted lower with increasing etching time, due to the removal of amorphous regions including folds and less-perfect crystals, as has been observed in oriented PE[25]. The significant decrease in T_m is ascribed to a limited initial crystal thickness, the lowering of M_v, and the suppression of reorganization during the d.s.c. heating scans, as detailed later. Concurrent with these changes, the ΔH_f increased gradually.

The d.s.c. thermograms from the second run for the initial powders, after melting and recrystallization, showed a significantly broader melting peak at a lower temperature (135°C). However, highly etched samples showed only minor changes in T_m and ΔH_f on the first and second runs, due to the formation of chain-extended crystals.

Figure 3 shows the variations in χ_c estimated from the ΔH_f for the first heating scans with treatment time for the reactor powder series polymerized at different T_{poly} in the range 20–90°C. On short-time etching (1 month or less), χ_c increased more rapidly with etching time for the powders polymerized at a higher T_{poly} (samples 4 or 5) than for the samples prepared at a lower T_{poly}. On further treatment, χ_c increased slowly and approached a maximum value of around 85–95% on etching for over 12 months for each of the reactor powders. The maximum χ_c value depended on the T_{poly}. For a given etching time, a higher crystallinity was obtained for the powder prepared at a higher T_{poly}, revealing a higher accessibility of the amorphous regions to the fuming nitric acid etching. This indicates that nitric acid could diffuse more rapidly within the powder prepared at a higher T_{poly}, suggesting a looser chain packing in its amorphous regions than for the powder prepared at a lower T_{poly}.

The maximum saturated ΔH_f values are slightly lower than that of a perfect PE crystal. A similar result has been previously reported for the mild etching of PP samples[26]. Such a low limit of the ΔH_f for fully etched samples results primarily from the formation of $-NO_2$ and $-COOH$ groups at the chain ends[21]. Indeed, the density of a powder polymerized at 80°C and etched for 24 months was over 1.000 g m^{-3}, the crystal density of PE. The increase in sample density due to the heavy chain end groups caused a

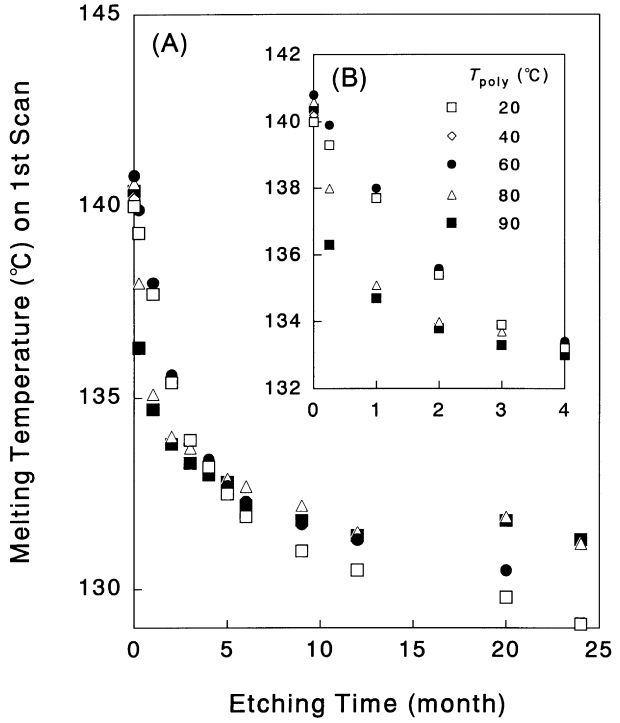

Figure 4 D.s.c. peak melting temperature for the first run *versus* etching time for a series of UHMW-PE reactor powders. (A) Over the whole etching time-scale. (B) Enlargement of the short-time scale up to 4 months

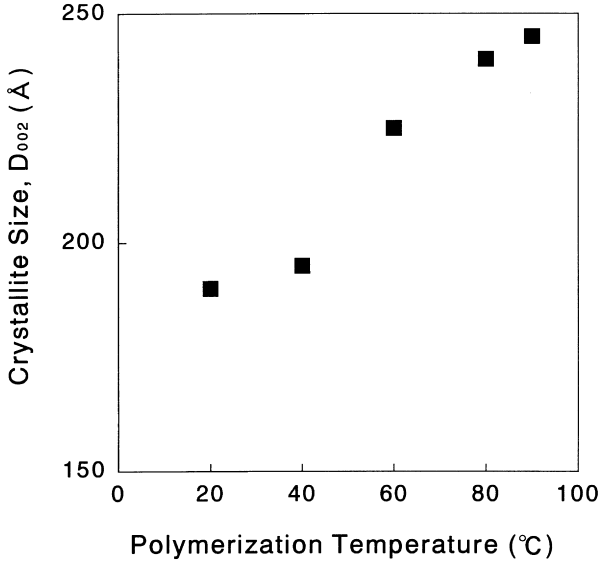

Figure 5 WAXD crystallite size along the chain axis, D_{002}, *versus* polymerization temperature for a series of un-etched reactor powders

decrease in the amount of PE per unit weight. The enthalpy in the melt also decreased due to the interactions between these end groups[27]. Further, the depression of T_m for the treated samples (see *Figure 4*) produced a decrease in the observed ΔH_f. These morphological features of etched samples are consistent with the decrease in ΔH_f (χ_c) of fully etched samples with decreasing T_{poly} (*Figure 3*) due to their smaller crystal thickness, as discussed below.

Figure 4 shows the changes in T_m with treatment time for d.s.c. first runs for the same series of reactor powders as in *Figure 3*. For the untreated samples, no significant differences were observed in the peak T_m values, as well as in ΔH_f (χ_c in *Figure 3*). The changes on etching for shorter times (4 months or less) are enlarged, and are shown in *Figure 4B*. The T_m of the powders polymerized at higher T_{poly} decreased more rapidly with increasing etching time than those prepared at lower T_{poly}, which is clearly observed in *Figure 4B*. However, such a decrease in T_m became gradually insignificant, and T_m approached a constant on prolonged etching (over 12 months). The T_m of a fully etched powder is slightly higher for the powder prepared at a higher T_{poly}.

The etching rate, evaluated from the depression in T_m, may be affected by the initial crystal thickness and the diffusion rate of nitric acid within the amorphous regions. For a constant crystallinity and diffusivity of the acid, the etching rate may be expected to be faster for a sample consisting of thinner crystals, since the latter has a wider total surface area accessible to nitric acid. However, the results in *Figure 4* show that the samples prepared at higher T_{poly} and consisting of thicker crystals were etched more rapidly than those prepared at lower T_{poly} and having thinner crystals. As discussed above (*Figure 3*), this also suggests that the diffusion rate of the acid within the amorphous regions plays a predominant role in determining the etching rate, and was significantly slower for the samples prepared at lower T_{poly}, reflecting the characteristics of their amorphous regions.

Generally, the d.s.c. T_m can be a measure of the crystal thickness, if structural reorganization does not occur during heating[28]. Independently of T_{poly}, the reactor powders exhibited a high T_m of 140–141°C, which is close to the T_m of a chain-extended PE crystal[21]. However, the T_m values for fully etched samples were in the range 128.8–131.5°C, significantly lower than the values for the initial powders. This indicates that the crystal thickness of the reactor powders is not as large as that estimated from a T_m of about 140°C, and a higher T_m is a result of rapid reorganization during heating. A similar conclusion has been reported[29,30]. Such a crystalline rearrangement requires chains sliding past each other within a crystal, which may easily occur in the reactor powders due to fewer entanglements on the lamellae surfaces. However, such lamellar thickening is impossible for fully etched samples, consisting of chain-extended crystals. Thus, the T_m of an etched sample is directly related to the crystal thickness of the nascent powder. To confirm this, the crystallite thicknesses along the chain axes, D_{002}, for the nascent samples were measured by WAXD analysis, and compared to the T_m for each of the samples fully etched by fuming nitric acid.

Figure 5 shows D_{002} as a function of T_{poly} for the series of reactor powders. With increasing T_{poly}, D_{002} increased, consistent with the increase in T_m for the fully etched samples. Parker *et al.*[31] have also observed a similar effect of T_{poly} on the lamellar thickness by performing neutron scattering studies on PE reactor powders. Such dependence of the crystal thickness on T_{poly} suggests that the crystallization occurred near T_{poly}, after the segmental length of a growing chain had reached a certain value during polymerization. The critical segmental length is likely to be longer at higher T_{poly}, as suggested by a larger crystal thickness for a sample prepared at a higher T_{poly}. Further, the activities of the catalyst sites were not uniform for the high-activity Ziegler catalyst used in this work, thus producing different segmental lengths before crystallization took place[17]. Crystallization under these conditions is most likely to provide an opportunity for the formation of

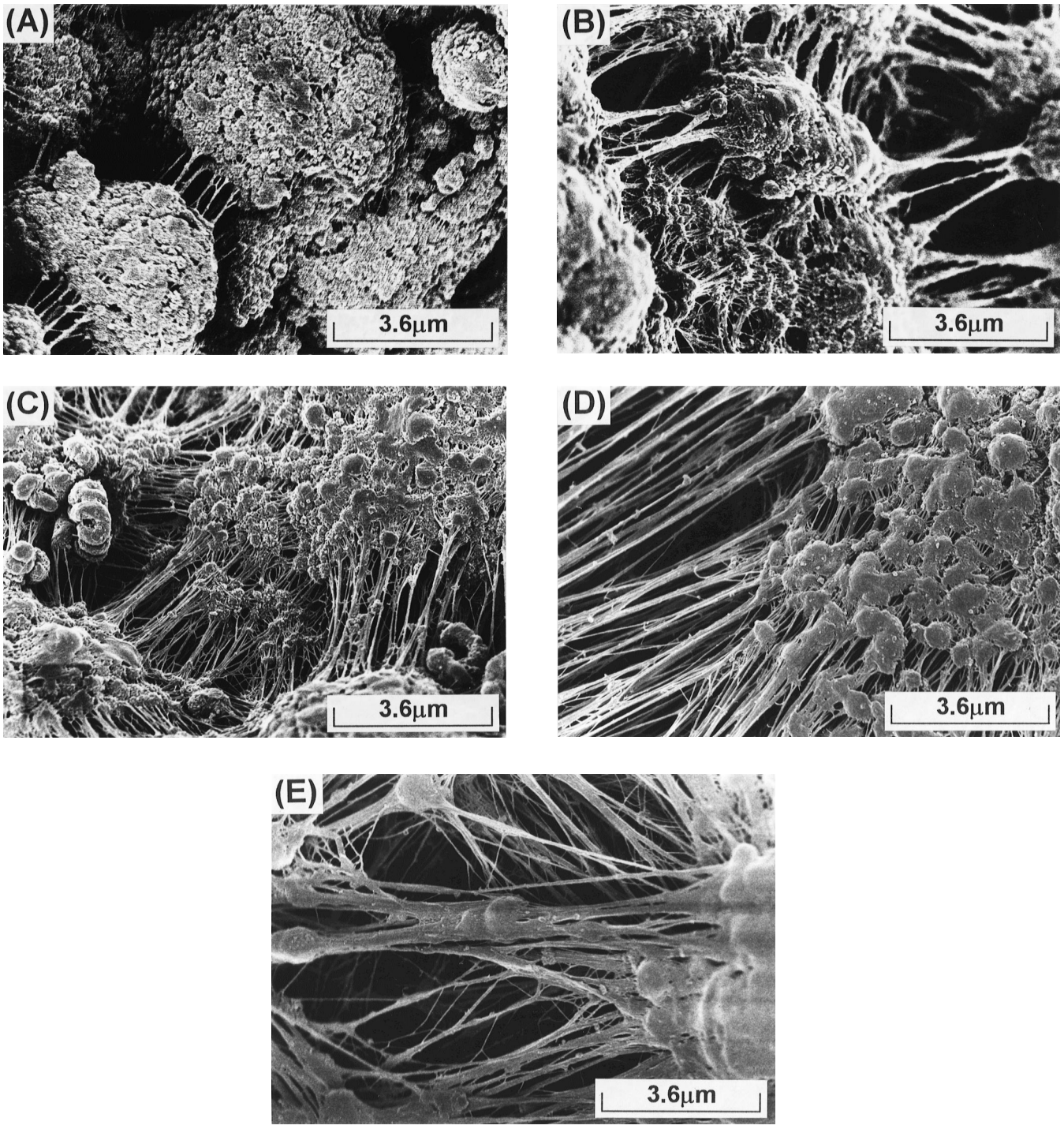

Figure 6 Scanning electron micrographs of a series of untreated reactor powders, prepared at different T_{poly}. (A) Sample 1 (20°); (B) sample 2 (40°C); (C) sample 3 (60°C); (D) sample 4 (80°C); (E) sample 5 (90°C)

entanglements by the diffusion of segments with different lengths. These entanglements include the classical ones and the latent entanglements recently proposed by Ottani and Porter[32]. Such an opportunity may be more prominent at a higher T_{poly}, since crystallization occurs after the length of the growing segment during polymerization has exceeded a certain value, which increases with T_{poly}, and segmental diffusion is more active at a higher T_{poly}.

SEM observations

To examine the morphologies of these powders, SEM observations were made on both the nascent and the etched samples. *Figure 6* shows SEM images for the nascent powder series. The powder with particles 100–150 μm in diameter prepared at 20°C (sample 1) consists of globular particles with a diameter of 2–5 μm. A few extended fibrils (about 40 nm wide and about 1 μm long) connecting these particles, are also observed (*Figure 6A*). The numbers and sizes of the extended fibrils (40–150 nm wide and 2–10 μm long) significantly increased as T_{poly} increased. The origin of such a fibrous structure is thought to be the internal expansion stress, which increases during polymerization[18,19]. The activity of the catalyst sites is accelerated by the increasing T_{poly}. Thus, polymer chains grow rapidly on the catalyst surface inside the particles, causing an expansive force on the previously deposited polymer.

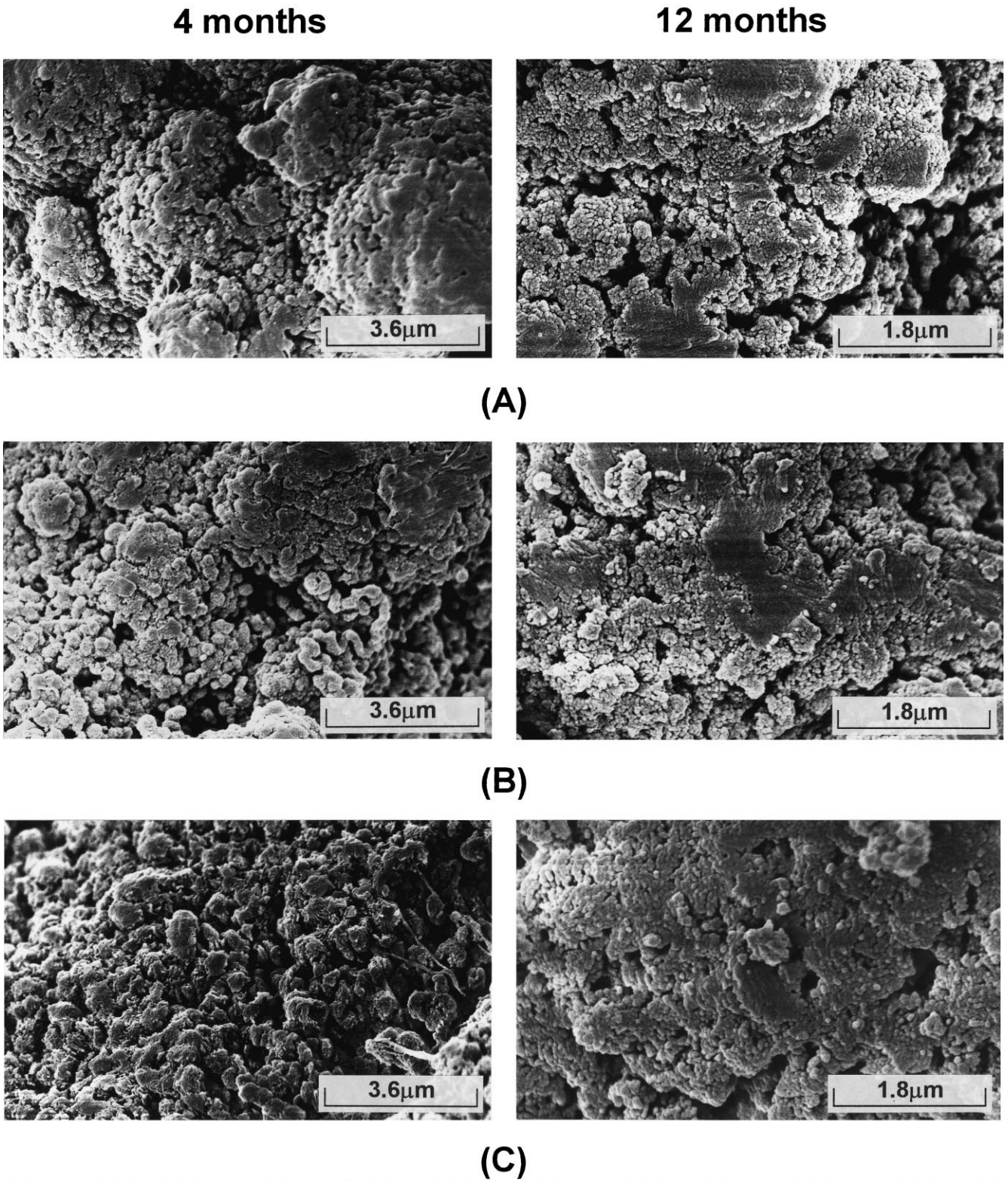

Figure 7 Scanning electron micrographs showing the changes in powder morphology on etching for a series of reactor powders prepared at different T_{poly}. (A) Sample 1 (20°C); (B) sample 2 (40°C); (C) sample 4 (80°C). The micrographs on the left- and right-hand sides were obtained after etching for 4 months and 12 months, respectively.

With the particle radius increasing as the synthesis proceeds, the outer polymer membrane is stretched, producing the extended fibrils connecting the particles. These SEM observations show that the microstructure of nascent powders significantly depends on their T_{poly}, which was also suggested by their drawability (*Figure 1*) and melting behaviour after etching (*Figures 2–4*).

The etched morphologies of the series of reactor powders were also examined by SEM. For the shorter etching time of 1 month, the morphologies changed only slightly. Small, extended fibrils disappeared, and larger ones survived (not shown). *Figure 7* shows SEM micrographs of the powder series etched for 4 and 12 months. On etching the powders for 4 months, the extended fibrils disappeared for all the

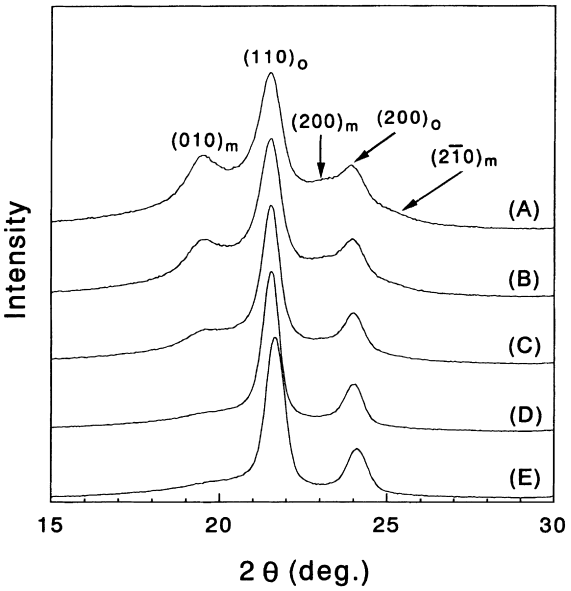

Figure 8 WAXD profiles for a series of UHMW-PE reactor powders prepared at different T_{poly}. (A) Sample 1; (B) sample 2; (C) sample 3; (D) sample 4; (E) sample 5

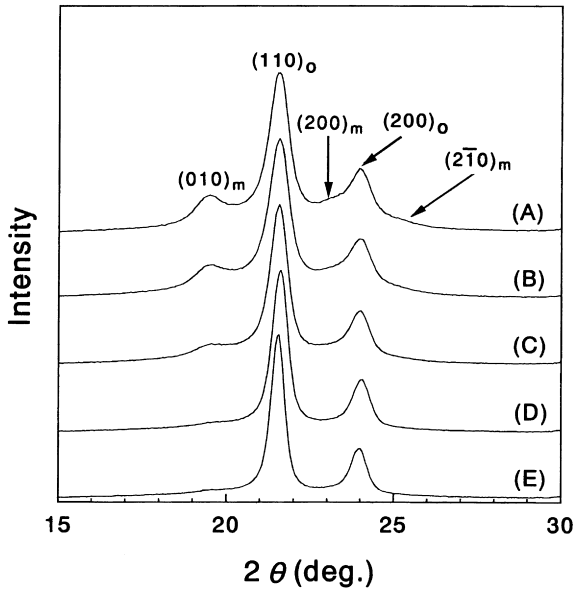

Figure 9 WAXD profiles for a series of UHMW-PE reactor powders etched for 9 months by fuming nitric acid at room temperature. The samples (A)–(E) are the same as in *Figure 8*

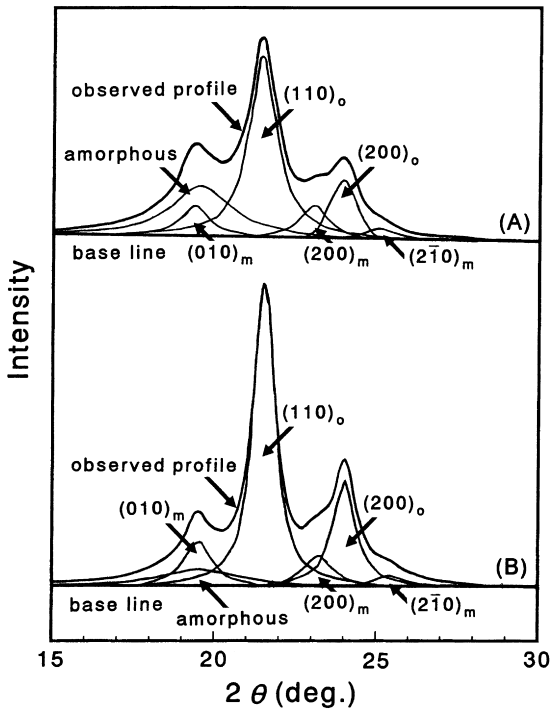

Figure 10 Decomposition of the WAXD patterns of a reactor powder prepared at $T_{poly} = 20°C$, (A) before and (B) after etching for 9 months

samples. On further etching for 12 months, the boundaries between the structural units became clearer, due to their shrinkage by the selective removal of the amorphous components.

These results reveal that the extended fibrils are highly accessible to fuming nitric acid. This is likely to be due to the fibrils observed by SEM being exposed at the powder particle surface and kept in contact with fresh nitric acid. The amorphous components of the powder polymerized at a lower T_{poly} are etched more slowly (see *Figure 1*), suggesting a slower diffusion of nitric acid in the amorphous regions due to the higher amorphous density. In contrast, the amorphous regions of the powder prepared at higher T_{poly} are likely to have a looser chain packing, as suggested by the more rapid etching. These structural features are likely to be related to the lower ductility of the nascent powder polymerized at a higher T_{poly}, as discussed in a previous section on the formation of entanglements during polymerization.

The crystalline forms of these powders were also analyzed by WAXD. *Figure 8* compares the WAXD patterns for the nascent powder series. The orthorhombic reflections are dominant for all powders. However, a monoclinic $(010)_m$ peak was clearly observed at $2\theta = 19.5°$ for the samples prepared at lower T_{poly}. In the WAXD patterns of samples with a lower T_{poly} (*Figure 8A*), a weak monoclinic $(200)_m$ reflection also appeared between the orthorhombic $(110)_o$ and $(200)_o$ reflections. Another monoclinic $(2\bar{1}0)_m$ reflection was observed as a shoulder on the higher-angle side of the $(200)_o$ reflection. The relative

intensity of these monoclinic reflections decreased with increasing T_{poly}. For the powders polymerized at 80 and 90°C (*Figure 8D* and 8*E*), no monoclinic reflections are observed, and all crystals are in the orthorhombic modification. Such a monoclinic modification is often formed on cold drawing of PE[33]. Thus, stress relaxation often causes a transition from the deformed monoclinic to the normal orthorhombic form[34]. Also, it is reported that the monoclinic crystals easily transform into the normal orthorhombic crystals on annealing[35–37]. However, this crystalline phase transition is undetectable by d.s.c. because of the small difference in enthalpy between these two crystalline forms.

The etched sample morphologies were also characterized by WAXD. *Figure 9* shows WAXD patterns for the same powder series as in *Figure 8*, but etched for 9 months. A comparison of *Figures 8 and 9* shows a significant decrease in intensity of the broad amorphous halo centred around $2\theta = 19.6°$, after 9 months of etching (*Figure 9*). Further, the intensities of the monoclinic peaks seem not to change on prolonged etching.

To show these features clearly, the decomposition of the patterns in *Figures 8A* and *9A* into orthorhombic and monoclinic reflection peaks and the amorphous halo was carried out by assuming a symmetrical function consisting of Gaussian and Lorentzian profiles with appropriate proportions for each of the peaks, as shown in panels A and B, respectively, in *Figure 10*. Further, for the decomposition, the amorphous halo profile at room temperature was assumed to be the same as that observed for a molten UHMW-PE film at 160°C, and the peak position only of the latter was shifted to the $2\theta = 19.6°$ reported for the former[24]. The amorphous halo seen in *Figure 10A* almost disappeared, and crystalline reflections were emphasized on etching (*Figure 10B*). The weak monoclinic $(200)_m$ and $(2\bar{1}0)_m$ reflections, which were ambiguous in the original profile, are clearly seen around $2\theta = 23.1°$ and $2\theta = 25.2°$, respectively. Furthermore, the relative amounts of the monoclinic and the orthorhombic forms were unchanged even after prolonged etching (more than 9 months). These facts confirm that the amorphous regions of the reactor powders were selectively removed and the crystalline phases remained after the long-time treatment, independent of the crystal modification.

CONCLUSIONS

The ductility of nascent UHMW-PE reactor powders, prepared with use of a high-activity Ziegler catalyst and having comparable M_v values of 2×10^6, depends significantly on T_{poly}. The drawability of the powders increased with decreasing T_{poly}. Direct SEM observations of the nascent powders showed that each powder (sized 50–150 μm) consisted of globular particles 2–5 μm in diameter and extended fibrils 40–150 nm wide and 1–10 μm long connecting these particles. The powders polymerized at higher T_{poly} values exhibited larger amounts of such fibrils. During gentle etching by fuming nitric acid at room temperature, the extended fibrils disappeared rapidly. On further etching, the boundaries between the different structures became clearer, due to their shrinkage by the selective removal of amorphous regions. WAXD measurements clearly showed that both orthorhombic and monoclinic crystals remained in the same ratio even after a long treatment time (more than 9 months).

The d.s.c. melting behaviour of the nascent powders showed no significant dependence on T_{poly}, primarily due to rapid reorganization during the d.s.c. heating scans. However, the melting endotherms of etched samples were significantly influenced by T_{poly}, reflecting variations in the nascent morphology with T_{poly}. On etching, both T_m and ΔH_f changed more rapidly for the sample polymerized at a higher T_{poly}. This indicates that the amorphous region of nascent powders prepared at higher T_{poly} is more accessible to chemical etching. Further, the T_m of fully etched samples increased with T_{poly}, revealing an increase in the crystal thickness with T_{poly}. This suggests that crystallization during polymerization occurred after the growing polymer chains had reached a certain length, which might increase with T_{poly}. The activity of the catalyst sites is not uniform and increases with T_{poly}, and segmental diffusion is more active at a higher T_{poly}. Thus, crystallization during polymerization at higher T_{poly} most likely provides more opportunity for the formation of entanglements due to segmental diffusion before the crystallization takes place. The effect of T_{poly} on the ductility of nascent UHMW-PE is likely to be related to the different microstructures in the amorphous regions formed during polymerization under different conditions.

REFERENCES

1. Smith, P., Lemstra, P. J., Pijpers, J. P. L. and Keil, A. M., *Colloid Polym. Sci.*, 1981, **259**, 1070.
2. Kanamoto, T., Zachariades, A. E. and Porter, R. S., *Polymer*, 1994, **35**, 4976.
3. Smith, P., Lemstra, P. J. and Booij, H. C., *J. Polym. Sci., Polym. Phys. Ed.*, 1981, **19**, 877.
4. Kanamoto, T., Tsuruta, A., Tanaka, K., Takeda, M. and Porter, R. S., *Macromolecules*, 1988, **21**, 470.
5. Sakurada, I., Ito, T. and Nakamae, K., *J. Polym. Sci., Part C*, 1966, **15**, 75.
6. Kanamoto, T., Tsuruta, A., Tanaka, K., Takeda, M. and Porter, R. S., *Polym. J.*, 1983, **15**, 327.
7. Kanamoto, T., Ohama, T., Tanaka, K., Takeda, M. and Porter, R. S., *Polymer*, 1987, **28**, 1617.
8. Griswold, P. D., Zachariades, A. E. and Porter, R. S., *Polym. Eng. Sci.*, 1978, **18**, 861.
9. Watanabe, M., Mizorogi, K., Uehara, H., Kanamoto, T., Sano, A. and Matsuura, K., *Rep. Prog. Polym. Phys. Jpn.*, 1993, **36**, 285.
10. Uehara, H., Kanamoto, T., Murakami, S. and Kawaguchi, A., *Macromolecules*, 1996, **29**, 1540.
11. Smith, P., Chanzy, H. D. and Rotzinger, B. P., *Polym. Commun.*, 1985, **26**, 258.
12. Smith, P., Chanzy, H. D. and Rotzinger, B. P., *J. Mater. Sci.*, 1987, **22**, 23.
13. Rotzinger, B. P., Chanzy, H. D. and Smith, P., *Polymer*, 1989, **30**, 1814.
14. Wang, L. H., Ottani, S. and Porter, R. S., *Polymer*, 1991, **32**, 1776.
15. Kanamoto, T. and Ito, M., *Polym. Prepr. Jpn.*,, 1991, **40**(4).
16. Blais, P. and Manley, R. St. John, *J. Polym. Sci. Part. A-1*,, 1968, **6**, 291.
17. Keller, A. and Willmouth, F. M., *Makromol. Chem.*, 1969, **121**, 42.
18. Graff, R. J. L., Kortleve, G. and Vonk, C. G., *J. Polym. Sci. Polym. Lett.*, 1970, **8**, 735.
19. Chanzy, H. D., Revol, J. F., Marchessault, R. H. and Lamandé, A., *Kolloid-Z. Z. Polym.*, 1973, **251**, 563.
20. Hoetchst Plastics, Catalog of Hostalene GUR (UHMW-PE), 1989.
21. Wunderlich, B., Crystal Structure, Morphology, and Defects, in *Macromolecular Physics*, Vol. 1. Academic Press, New York, 1973.
22. Illers, K. H., *Makromol. Chem.*, 1968, **118**, 88.
23. Wunderlich, B. and Cormier, C. M., *J. Polym. Sci., Part A-2*,, 1967, **5**, 987.
24. Klug, H. P. and Alexander, L. E., *X-ray Diffraction Procedures*. John Wiley and Sons, New York, 1974.
25. Weeks, N. E. and Porter, R. S., *J. Polym. Sci., Polym. Phys. Ed.*, 1975, **13**, 2049.
26. Uehara, H., Yamazaki, Y., Otake, C. and Kanamoto, T., *Koubunshi Ronbunshuu*, 1994, **51**, 597.

27. Okui, N., Narita, N., Shimada, T. and Kawai, T., *Koubunshi Ronbunshuu*, 1974, **31**, 469.
28. Hoffman, J. and Weeks, J. J., *J. Res. Natl. Bur. Std.*, 1962, **66A**, 130.
29. Ottani, S. and Porter, R. S., *J. Polym. Sci. Polym. Phys. Ed.*, 1991, **29**, 1179.
30. Engelen, E. Y. M. T. and Lemstra, P., *J. Polym. Commun.*, 1991, **32**, 343.
31. Parker, S. F., Maddams, W. F., Vickers, M. E., Williams, K. P. J. and Downs, G. W., *Polymer*, 1996, **37**, 2755.
32. Ottani, S. and Porter, R. S., *Makromol. Chem., Rapid. Commun.*, 1996, **16**, 813.
33. Kawaguchi, A., Murakami, S., Katayama, K., Mihoichi, M. and Ohta, T., *Bull. Inst. Chem. Kyoto Univ.*, 1991, **69**, 145.
34. Steidl, J. and Peizbauer, Z., *J. Polym. Sci., Part. C*, 1972, **38**, 345.
35. Seto, T., Hara, T. and Tanaka, K., *Japan J. Appl. Phys.*, 1968, **7**, 31.
36. Nakayama, K. and Kanetsuna, H., *J. Mater. Sci.*, 1975, **10**, 1105.
37. Takahashi, Y., Ishida, T. and Furusaka, M., *J. Polym. Sci., Part. B*, 1988, **26**, 2267.